This manuscript was published as formal in:

Liquid Crystals, Volume 43, 2016 - Issue 13-15, Pages 1973-1985

https://doi.org/10.1080/02678292.2016.1172353

https://www.tandfonline.com/doi/full/10.1080/02678292.2016.1172353

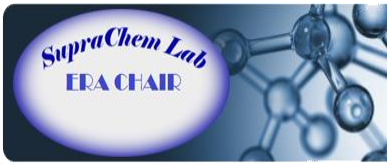

Title:

PDLC composites based on polyvinyl boric acid matrix – a promising pathway towards biomedical engineering

by:

Daniela Ailincai[1], Cosmin Farcau[2], Elena Paslaru[1], Luminita Marin[1]*

[1]"Petru Poni" Institute of Macromolecular Chemistry, Aleea Grigore Ghica Voda 41A,Iasi, 700487, Romania

[2] Babes- Bolyai University, Nanobiophotonics and Laser Microspectroscopy Center, 42 Treboniu Laurian, 400271 Cluj-Napoca, Romania.

*Corresponding Author: Luminita Marin

e-mail: lmarin@icmpp.ro

Abstract

Polymer dispersed liquid crystal (PDLC) systems based on a new smectic liquid crystal embedded into polyvinylalcohol-boric acid (PVAB) as biocompatible carrying matrix were prepared and characterized. The new smectic liquid crystal contains biologically friendly structural blocks and it was designed to have a direct isotropic-smectic transition and a mesophase stability range at human body temperature. The resulted PDLCs were characterized from morphological and thermotropic point of view by polarized light microscopy (POM), differential scanning calorimetry (DSC), scanning electron microscopy (SEM) and Raman microspectroscopy and their surface properties were determined by contact angle measurements and surface energy calculations.

It was concluded that the electron deficient PVAB matrix constrains the ester liquid crystal to grow as spherical droplets with planar anchoring. The droplet diameter was comprised in the range 4 – 11 μm, with predominant droplet population around 7 μm and narrower polydispersity as the liquid crystal amount into polymeric matrix increases. The resulted PDLC films exhibited versatile morphology and surface properties which allow targeting their application.

Keywords: polymer dispersed liquid crystals; polyvinyl alcohol boric acid; smectic droplets; contact angle; surface free energy

1.Introduction

Polymer dispersed liquid crystal (PDLC) systems are a relative new type of composite materials consisting in micrometric dispersion of liquid crystal (LC) droplets into a polymer matrix. Thus, they combine the unique optic properties of liquid crystals, different by the isotropic compounds, with film forming ability and mechanical strength of the polymer matrix. The development of PDLC composites actually started once their potential as active substrate in displays has been evidenced [1]. Applications as smart windows, holographic systems, micro-lens or lasers, kept the researchers interest in this challenging domain which grew continuously [2-6]. Today, the researcher attention goes to the potential applying of PDLCs in biomedical engineering and food industry: smart food packaging [7], artificial iris [8, 9], bio-sensors for biologically active matter [10] or other some envisaged bio-applications [11]. Such innovative bio-applications claim biocompatible materials. This is the reason why, the ability of biopolymers or biocompatible polymers to act as polymer matrix for PDLC composites is of current interest. In this context, our attention was attracted by the

polyvinylalcohol-boric acid (PVAB), a biocompatible polymer generally less studied, which keeps the promise to replace the well-known polyvinylalcohol. PVAB is soluble only in hot water, transparent and immiscible with liquid crystals, assuring good optical properties. One of our previous studies demonstrated that PVAB, due to its electron deficient boron atom, assures selective nematic liquid crystal anchoring without orientation defect and narrow LC droplet polydispersity – two very important attributes of the PDLC systems, usually difficult to be attain [12].

Among the PDLC systems, those containing smectic liquid crystals were demonstrated to be more attractive due to their high contrast, energy saving nature and ability to generate bistability - property which prompts the maintaining of optical states without an electrical field, being ideal for portable electronic devices. Moreover, the smectic A based PDLC composites demonstrated reversible memory attributed to the stiffness of the layer structure of the mesophase [13-16]. However, there are only few studies related to the PDLC composites based on smectic liquid crystals reported in literature, because of the difficulty in obtaining smectic liquid crystals with direct isotropic-smectic transition and large stability range at room temperature on a hand, and due to difficulty to grow smectic droplets in polymer matrix on another hand [17-20].

A literature survey reveals that ester containing liquid crystals are biological friendly compounds which are successfully used in bio-applications [21-23]. On the other hand, the known ester based smectic liquid crystals have high thermal transitions and thus high temperature mesophase stability range, property which make them unattractive for PDLC obtaining.

From all the above reasons, we decided to obtain new PDLC composites using PVAB as confinement matrix and a novel smectic liquid crystal with a direct smectic-isotropic transition and large mesophase stability range on the human body temperature domain, designed and synthesized by us [24]. Microencapsulation method was used in order to obtain initial composite films which microstructure has been reseted by thermal annealing. Complementary methods were used to characterize the novel PDLCs – polarized light microscopy, differential scanning calorimetry, scanning electron microscopy, Raman micro-spectroscopy, UV-vis and photoluminescence spectroscopy and contact angle measurements and surface energy calculations, – in order to access multiple scales involved in PDLC obtaining phenomena.

Three important aspects must be underlined here: (i) the smectic liquid crystal used in this study was designed and synthesised by us; (ii) PVAB is a versatile, less known and used biocompatible polymer (iii) the intrinsic valuable results obtained for the understudy PDLC composites can be used as model for encapsulation of ester based drugs into PVAB in view of controlled delivery.

2.Experimental

2.1.Materials

Polyvinyl alcohol boric acid (Mw=54 000, 4% water content) was purchased from Aldrich and used as received.

Buthyl-p-[p'-n-octyloxy benzoyloxy]benzoate (**BBO**) has been synthesised as smectic A liquid crystal with a direct isotropic-smectic A transition [24]. The benzoate derivative has been chosen as it is well known that benzoate derivatives are biologically and pharmacologically bioactive molecules – being useful for medical and analytical fields [23].

2.2.Synthesis

The smectic liquid crystal has been synthesized according to a published procedure [24]. Shortly, the p-hydroxy benzoic acid was transformed into p-octyloxy-benzoyl chloride via Williamson etherification to give p-octyloxy-benzoic acid followed by its treatment with thionyl chloride. Further, the final product buthyl-p-[p'-n-octyloxy benzoyloxy]benzoate (**BBO**) was obtained by reaction of the obtained benzoyl chloride with p-hydroxy buthyl benzoate. The crude product has been recrystallized from ethyl acetate when fine white single crystals suitable for X-ray crystallographic studies were successfully grown.

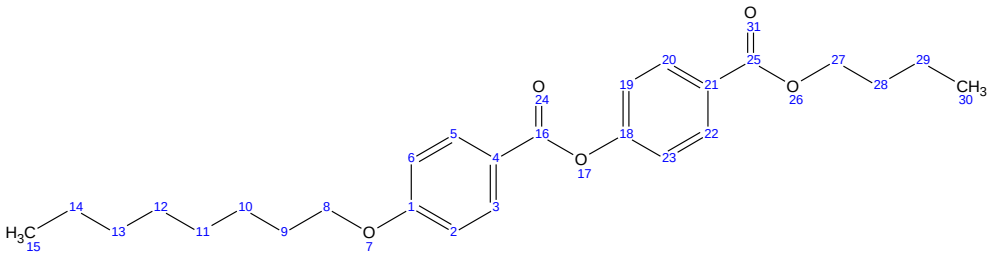

^{1}H-NMR (400.13 MHz, DMSO-d_6, ppm) δ = 8.11, 8.09 (d, 2H, H3,5); 8.08, 8.06 (d, 2H, H20,22); 7.47, 7.45 (d, 2H, H19, 23); 7.15, 7.13(d, 2H, H2, 6); 4.33, 4.32, 4.30 (t, 2H, H27); 4.13, 4.11, 4.10 (t, 2H, H8); 1.79, 1.77, 1.75, 1.73, 1.71 (m, 4H, H9, 28); 1.49, 1.47, 1.45, 1.44, 1.42 (m, 4H, H10, 29); 1.40 – 1.24 (overlapped peaks, 8H, H11, 12, 13, 14); 0.98, 0.97, 0.95 (t, 3H, H30); 0.90, 0.89, 0.87 (t, 3H, H15)

Crystal data: $C_{52}H_{68}O_{10}$ (M_r= 853.06 g·mol^{-1}), triclinic, *a* = 5.7447(6) Å, *b* = 14.5648(14) Å, *c* = 28.725(2) Å, α = 98.673(7)°, β = 94.343(7)°, γ = 91.478(8)°; *V* = 2367.4(4) Å^3, *T* = 160 K, space group *P*-1, *Z* = 2, 1652 coll. refl., 8053 indep. (R_{int} =0.0779), G_{of} = 1.000, R_1= 0.0935, wR(F^2))= 0.2132.

2.3.***Techniques***

^{1}H-NMR spectrum of **BBO** was recorded on a BRUKER Avance DRX 400 MHz spectrometer, equipped with a 5 mm direct detection QNP probe with z-gradients. The chemical shifts are reported as δ (ppm) relative to the residual peak of the DMSO solvent.

Crystallographic measurements on **BBO** single crystal were carried out with an Oxford-Diffraction XCALIBUR E CCD diffractometer using graphite-monochromated MoKα radiation, under the conditions described in the literature [24].

The textures of the pure liquid crystal and PDLC composites were observed by polarized light microscopy, with an Olympus BH-2 microscope equipped with a Linkam THMS 600/HSF9I heating stage and a TMS91 control unit. The samples were observed during a heating/cooling/heating scan, at a heating/cooling rate of 5 ^{o}C min^{-1}.

Differential scanning calorimetric (DSC) measurements were performed on a DSC 200 F3 Maia device (Netzsch, Germany), under nitrogen purge (nitrogen flow 50 mL/min). The device was temperature and sensitivity calibrated with indium, according to the standard procedures. Around 5 mg of each sample were loaded in punched and sealed aluminium crucibles and DSC curves have been registered on a heating-cooling-heating scan, at a heating/cooling rate of 5^o C min^{-1}. The transition temperatures were read at the top of the endothermic and exothermic peaks.

Raman spectra were collected on a confocal Raman microscope (WITec alpha300 R), under 532 nm laser excitation, a 0.9 NA objective, and a 100 μm pinhole. By using a 600 g/mm grating, the spectral region up to 3700 cm^{-1} can be recorded in a single spectrum, with a resolution of 3 cm^{-1}. Raman imaging was performed in scanning mode, with a resolution of ~31 pixels / μm^2. Raman images are constructed from the integrated intensity of a given Raman band, after background subtraction. The Raman system is equipped with an integrated polarization module, by which the polarization of the excitation beam can be rotated manually.

The microstructure of the composite films was viewed with a field emission scanning electron microscope (Scanning Electron Microscope SEM EDAX – Quanta 200) at accelerated electron energy of 10 eV. The morphological observation was carried out for (i)

the film samples as resulted by casting and for (ii) the films heated at 80 ^{o}C. The droplet diameters have been measured using Image J Software and the obtained values were further used to build the corresponding histograms using OriginPro 8 software.

The static contact angle for the PDLC and BBO film samples was obtained using a CAM-200 instrument from KSV Finland, by the sessile drop method, at room temperature and controlled humidity. The measurement was performed within 10 s after placing 1 μL drop of water on film surface and the contact angle was measured by fitting the drop profile using the Young-Laplace equation [12, 25]. The contact angle was measured on 5 random locations of the surface, the average value being considered. To calculate the components of the free surface energy and the total free surface energy, the contact angle at equilibrium between the studied surface and three pure liquids – twice distilled water, formamide and diiodomethane – was measured. The total surface free energy (γ_s^{TOT}) was calculated using the acid base approach of van Oss and Good [12, 25].

3.Results and discussions

3.1.*Smectic liquid crystal*

A thermotropic smectic liquid crystal containing ester linkages named buthyl-*p*-[*p*'-*n*-octyloxy benzoyloxy]benzoate] (**BBO**) has been synthesized by an esterification reaction starting from *p*-hydroxy benzoic acid [24]. The right structure of the liquid crystal has been proved by ^{1}H-NMR and Raman spectroscopy (Figure 1s) and further by single crystal X-ray diffraction measurements (**1**).

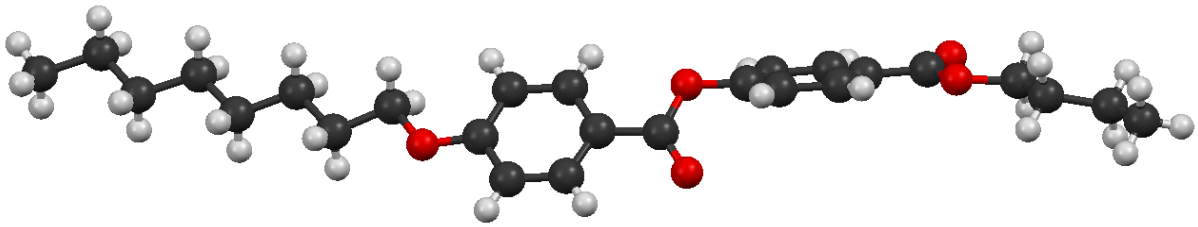

(1)

BBO

As can be seen, the **BBO** molecules adopt a twisted conformation conferred by the torsion of the ester linkage between the two aromatic rings. The driving force in supramolecular packing appears to be the rigid-flexible self-assembling (Figure 1) [26]. In the crystal structure, the molecules are packed forming ribbons with the intermolecular distance around 5.7 Å, extended parallel to the **a** axes. The ribbons are packed two by two forming

packs which lay in antiparallel directions along **b** axes and forming molecular layers. The inter-ribbons distance is quite short, around 3.5 Å, indicating strong lateral forces due to the hydrogen bonding between the neighbouring ester oxygens and aromatic or aliphatic hydrogens and also between the aromatic carbons and hydrogens. Further, along **c** axes, the molecular layers are arranged on antiparallel directions of the molecules, with the inter-layer distance around 9 Å. An important role in keeping the crystal integrity appears to be played by the strong lateral forces.

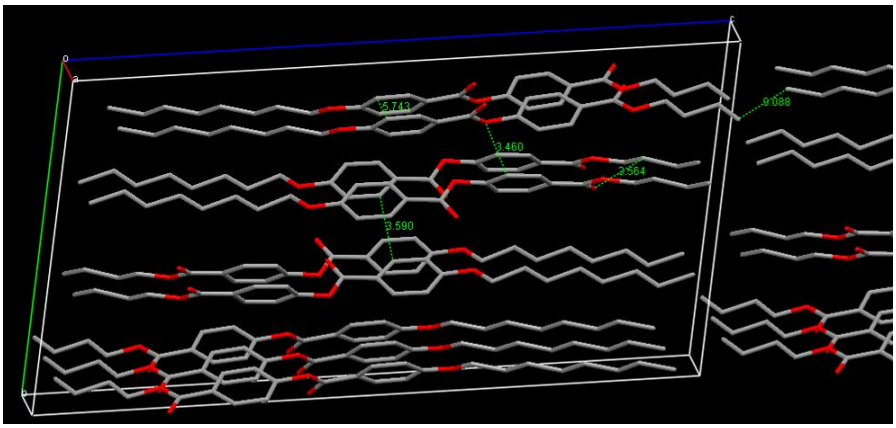

Figure 1. The packing of the **BBO** molecules to generate 3D structure

The thermotropic behaviour of the **BBO** compound, investigated by differential scanning calorimetry and polarized light microscopy, consists in the occurrence of an enantiotropic Smectic A mesophase with a direct isotropic- smectic A transition and a large mesophase stability range. As can be seen in figure 2, the smectic mesophase was observed during the heating scan by transition of the crystalline state into a striated marbled texture (Figure 2a), while during the cooling scan, it clearly appeared from isotropic state (Figure 2b) showing a characteristic fan-shaped texture [27, 28], which transformed into crystalline state at further cooling (Figure 2c).

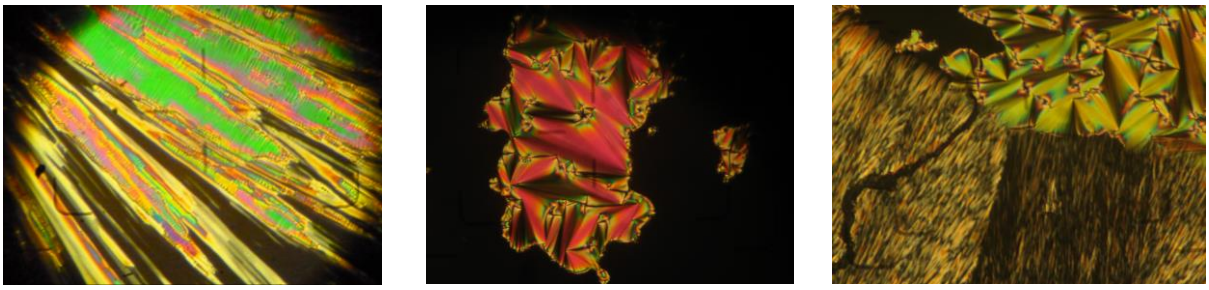

a) 1H, 55 ºC, Cr-Sm transition **b**) 1C, 72ºC, I-Sm transition **c**) 1C, 29 ºC, Sm-Cr transition

Figure 2. POM images revealing thermotropic behaviour of the **BBO** smectic liquid crystal **1H**: Cr 54 ºC SmA 73 ºC I; **1C**: I 72 ºC SmA 27 ºC Cr (H: heating, C: cooling)

Compared to cyano containing liquid crystals, generally used in PDLC obtaining, which were proved to be cytotoxic [29, 30], the new synthesized compound is built from biologically friendly building blocks [21, 23], having potential of use in bio-medical applications.

3.2.PDLC composites obtaining

PDLC composite films were obtained by encapsulation of the **BBO** smectic liquid crystal into polyvinyl alcohol boric acid as carrying matrix, *via* microemulsification method. The component ratio was varied to give four different samples with growing percent of liquid crystal, from 10 to 40 (Table 1). The composites gave free standing films, with high adhesivity to the glass support.

Table 1. Composition of the prepared PDLC composites

Code	**P1**	**P2**	**P3**	**P4**
% Sm	10	20	30	40
% PVAB	90	80	70	60

Polarized light microscopy, Raman microspectroscopy, differential scanning calorimetry, and scanning electron microscopy were employed in order to see the morphological characteristics of the new PDLC composites, in terms of droplet shape, size, polydispersity, distribution and configuration, as well as polymer anchoring effect and morphology stability. To further understand the interface forces at polymer – liquid crystal boundary, and in order to estimate the composite ability to be used as biomaterials, contact angle measurements and surface energy calculations were performed as well.

3.3.Polarized light microscopy

Polarized light microscopy (POM) is the visual method which allows a first simple determination of the liquid crystalline droplet segregation, and besides, provides two-dimensional information about their shape, location, size distribution and thermal dynamic in the observed plane. Comparing the pure LC thermotropic behaviour with that of the PDLCs, conclusions regarding the thermodynamic of the phase separation and especially the droplet anchoring principle can be drawn.

The pure smectic LC compound (**BBO**) exhibited in POM a clear fan shape texture, signature of a smectic **A** mesophase. The fan-shape texture is stable up to 28 ^{o}C when crystallizes.

As can be seen in figure 3a-c, the PDLC samples with smaller amount of LC showed clear round birefringent droplets. As the liquid crystal percent into the polymer matrix increases, the droplet density grows – an almost continuous fine birefringent texture being observed for the highest amount of LC, as result of the overlapped droplets on cross section of the transparent polymer matrix [12, 31, 32]. Generally, the colour within the droplets is distributed as concentric rings, similar to simple polygonal textures formed by smectic A mesophase in thick preparations [27].

During the heating, the crystalline-smectic transition wasn't seen, suggesting a pre-existent layered organization of the crystalline state (see crystallographic analysis) which was kept into the smectic mesophase also, and could be stabilized by the interphase interaction with polymer matrix. The droplet isotropization occured slowly on a larger temperature range (between 67 and 72 ^{o}C) compared to pure liquid crystal (between 69 and 70 ^{o}C), clearly indicating strong interphase forces able to anchor the liquid crystal droplets. Moreover, the isotropic LC droplets remained surrounded by a milky birefringent radial shadow (Figure 3d), indicating the organization of the polymer matrix at the interphase [12, 32]. The milky birefringence became more intense when the PDLC films were kept for a while, indicating that PVAB ordering around the **BBO** liquid crystal evolves during the time (Figure 3d'). So, it could be concluded that strong interactions between the electron deficient boron atom of the PVAB and the negative charged ester bonds of the **BBO** appeared, resulting in an ordering coupling at interface between the two phases. Consequently, taking into consideration the structure of the **BBO**, it could be estimated a parallel disposition of their molecules on the droplet wall.

During the cooling, the coloured droplets also appeared gradually. The droplets have pretty uniform size and distribution into the polymer matrix. No other phase transition was clearly seen, indicating a good stabilization of the organization of the LC molecules within the droplets.

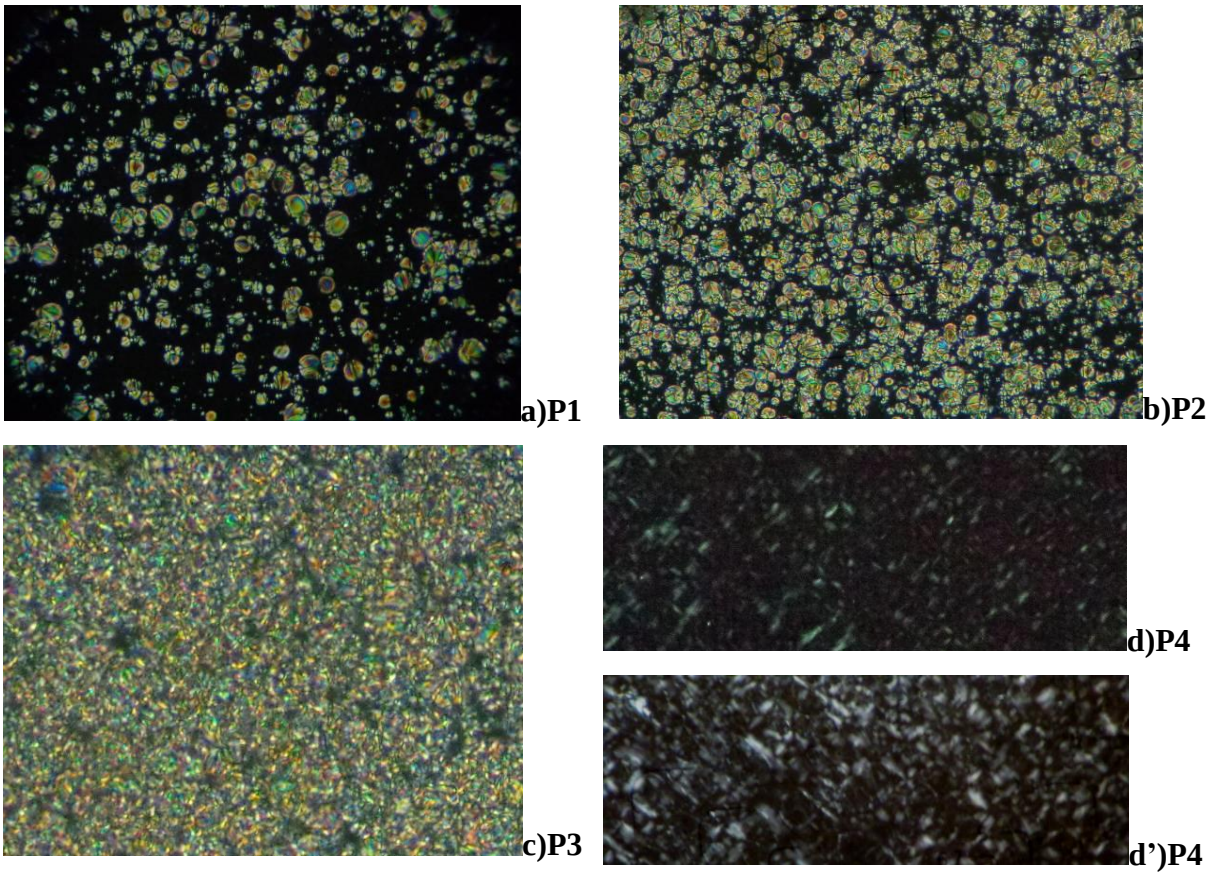

Figure 3. POM images of studied PDLCs, at room temperature, after the stabilization by TIPS treatment (a, b, c) and at 75 ^{o}C, when **BBO** is in isotropic state, 2 weeks after preparation (d) and 4 months after preparation (d')

This thermotropic behaviour suggested that, into the liquid crystalline droplets, a simple polygonal texture characteristic to thick LC samples took the place of the fan shaped texture formed by the pure liquid crystal, as a consequence of the thick LC sample embedded in the polymer matrix compared to thin LC sample between two lamellae. The most probably, within the droplets with polygonal texture, the smectic layers are arranged in Dupin cyclides [27] with the focal conics laying with ellipses on the plane of droplet wall and the summit of the corresponding cone of revolution in the droplet centre. The whole droplet volume is thus filled with these cones. The molecules inside the cones are oriented with long axes parallel with respect to the droplet wall, due to the strong tangential anchoring stabilized by the interphase forces. A topographic image of the **BBO** distribution inside the smectic droplets is shaped in figure 4.

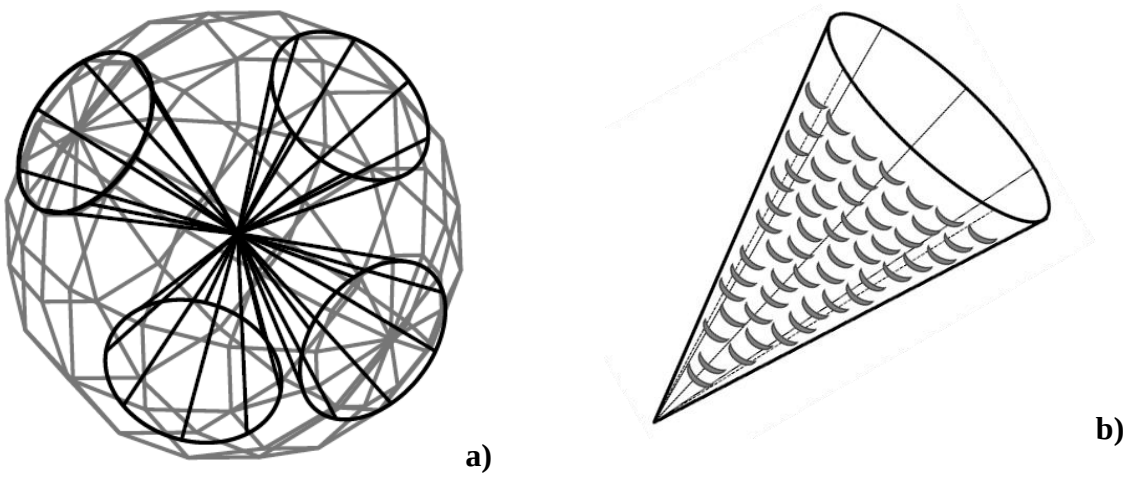

a) **b)**

Figure 4. a) Topology of the Smectic A polygonal texture into a droplet; b) inset on a focal cone with a parallel arrangement of the molecular axis on the cone ellipse

3.4.Raman microspectroscopy

Compared to POM, Raman microscopy provides a more detailed insight upon the spatial organization of the molecules inside the liquid crystal droplets. Besides, it is a valuable complementary method to establish the phase separation by mapping chemical composition [32]. The two pure composite components have own spectroscopic signature based on the different groups which vibrate at different wave number. Thus, while the Raman spectrum of the PVAB has the most important vibration bands due to the C-H stretching around 2800 cm^{-1}, the **BBO** liquid crystal has distinct bands due to the C=C stretching into the aromatic rings at 1600 cm^{-1} and COO group vibration at 1720 cm^{-1} (Figure 2s). Based on this different Raman signature, the composite mapping was realised, when different areas corresponding to a phase separation of the continuous polymer matrix and round liquid crystalline droplets appeared (Figure 5).

The **BBO** liquid crystal molecules are strong Raman scatterers. The vibration of the characteristic C=C and COO groups of the **BBO** compound occurs in the molecular plane and their vibration direction is parallel to the mean director direction [33]. As a consequence, they can be assimilated with orientational director **n** of the **BBO** smectic arrangement. The symmetric stretching of the C=C in the aromatic rings and stretching of the COO, respectively, have ability to induce major change of polarizability along the long molecular axis of the **BBO** molecules. As result, using liniar polarized laser beam, the average orientation of the **BBO** liquid crystal molecules can be evidenced by simple analysis of the two stretching bands. The intensity of these bands must be maximal when the electromagnetic

vector of the incident plane of polarized light (**P**) lies parallel to axis of the **BBO** molecules and minimal when lies perpendicular [32, 33]. Consequently, the orientational director which is more or less parallel to the long molecular axis can be found.

Figure 5 exhibits as an example, the Raman images of the **P2** composite together with Raman spectra registered for different areas (marked as 1, 2 and 3), at different orientations of the excitation laser polarization (**P**) as indicated by the double-arrow. The Raman maps are plotted from the intensity of the 1600 cm^{-1} Raman band.

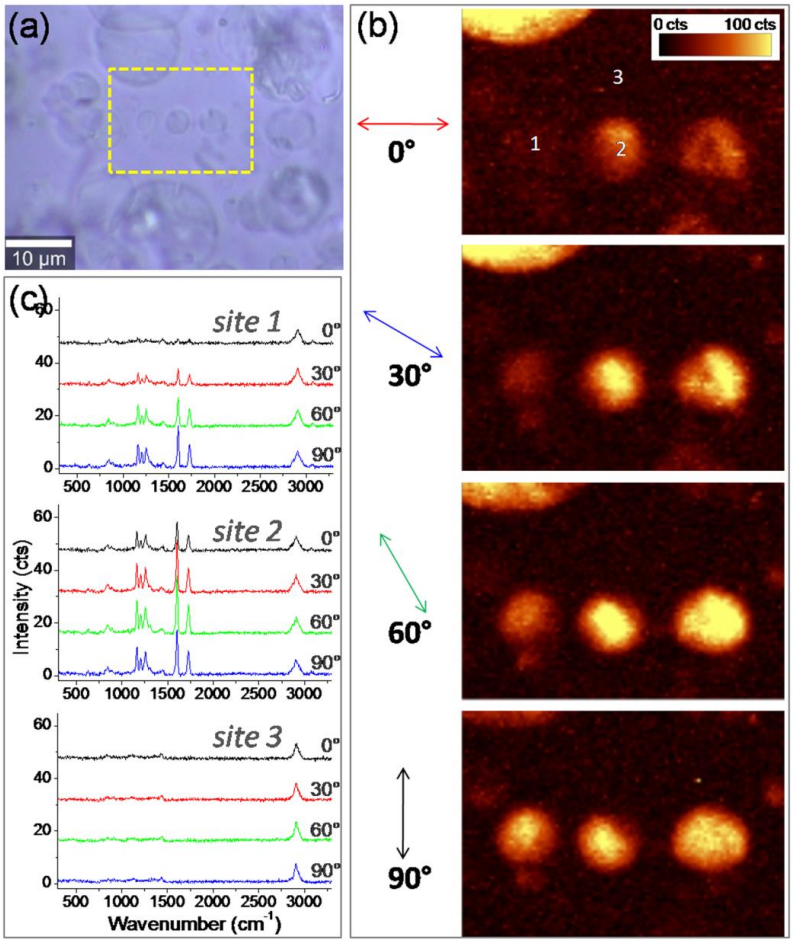

Figure 5. a) Bright-field optical microscopy image of the **P2** composite; b) Raman image obtained by plotting the intensity of the 1600 cm^{-1} **BBO** Raman band across the area marked by the rectangle in (a); c) Raman spectra collected at sites 1-3 (marked in (b)) for different polarizations of the excitation laser.

The preferential orientation of the **BBO** molecules was clearly evidenced by the dependence of the Raman band intensity on the polarization of the excitation laser. The variation occurred between a maximum to a complete missing of the bands, (Figure 5, case 1), or between a maximum and a minimum (Figure 5, case 2), indicating spherical droplets tilted

under different angles (Figure 2s). Taking into account that maximum intensity is obtained when **n** II **P** and minimum when **n** ⊥ **P**, it can be assumed that orientational director of the **BBO** has a radial orientation of the molecules inside of droplet, with long axis parallel to the droplet wall, reaching a tangential anchoring. A similar behaviour was observed also by plotting the Raman images corresponding to the 1720 cm^{-1} band. On the contrary, by plotting the Reighley band (laser scattering) or the Raman band at 2900 cm^{-1} (from the matrix) the dependence on laser polarization does not present the same behaviour (Figure 3s). This enforces our conclusion that by polarized Raman imaging the orientation of the molecules inside the droplets was indeed reached. Thus Raman spectroscopy undoubtedly confirmed the theoretical premises and POM observations, exhibiting that the smectic liquid crystal drops were strong planar/tangential anchored by the PVAB confining matrix, the drops being filled with focal conic domains in which the molecules have the orientational director planar to the boundary [34].

3.5.Differential scanning calorimetry

Differential scanning calorimetry (DSC) is an important technique in PDLC characterization, giving information about the LC segregation, transition dynamic, the droplet size polydispersity and also about the liquid crystal/carrying matrix miscibility and morphological stability of the composite materials.

Compared to pure LC, the DSC curves of the PDLC composites showed no important changes during the heating scans; the crystalline melting and smectic-isotropic transition occurred at the same temperature as pure liquid crystal (Figure 6a). Instead, important changes could be seen in the cooling scans (Figure 6b). First, the isotropic-smectic transition happend at lower temperature and the exothermic peak was larger indicating a slower occurrence of the smectic mesophase explained by the difficult organization of the molecules into the Dupin cyclides, constrained by their tangential anchoring to adopt exact positions inside the cones. Secondly, instead the broad exotherm resulted by superposing of two peaks (30 and 28 ^{o}C) of the pure liquid crystal, two well separated exothermic peaks appeared, indicating the separation of two clear transitions: SmA-SmX (31 ^{o}C) and SmX-crystalline (0 ^{o}C), where SmX is a higher ordered smectic mesophase. This clearly reflects the ability of the polymer matrix to stabilize the smectic mesophase, a more ordered smectic mesophase being stabilized up to ~ 0 ^{o}C against crystalline state.

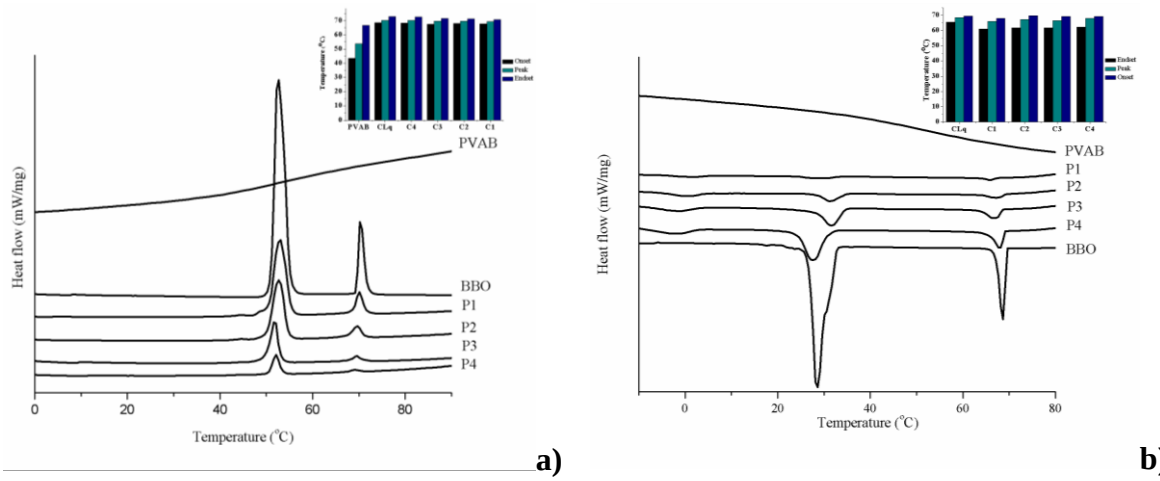

Figure 6. DSC curves of pure liquid crystal, PVAB and PDLCs during a) second heating and b) first cooling scan (inset: graphical representation of the smectic-isotropic endotherm and isotropic-smectic exotherm, respectively)

The exact reproduction of the DSC curves on many heating/cooling scans show the immiscibility of the **BBO** liquid crystal with the PVAB matrix and on hene the PDLC morphologic stability.

Comparing the DSC curves of the pure PVAB and PDLC composites, one can be observed that the second order transition around 60 ^{o}C of the pure PVAB corresponding to the glass transition (Tg), couldn't be seen in the case of the PDLCs, even by heating/cooling sample from room temperature up to 80 ^{o}C. The Tg absence suggests the enhancing of the ordering degree of the PVAB matrix into the PDLC composites – in agreement with POM observations, enforcing the conclusion that there is a ordering coupling at the liquid crystal-polymer matrix interface.

3.6.Scanning electron microscopy

To evaluate the microstructure of the PDLC composites, the film samples have been scanned at 10 keV, a) as obtained and b) preheated at 80 ^{o}C, to reach isotropic state of the liquid crystal.

The film samples show spherical shapes on the surface indicating spherical shape of the liquid crystalline droplets (Figure 7). Compared to other smectic LC based PDLCs, is remarkable the ability of PVAB matrix to constrain the smectic LC to adopt a round droplet shape instead of batonnets – characteristic to SmA mesophase [14]. Taking into consideration the tendency of the **BBO** liquid crystal to crystallize as needles either from solution (Figure

2a) or molten state (Figure 2d), the round droplets reflect the influence of the polymer matrix which exerts enough interface tension to prevent the needle like growth tendency and to determine a spherical confinement, during the liquid-liquid demixing process.

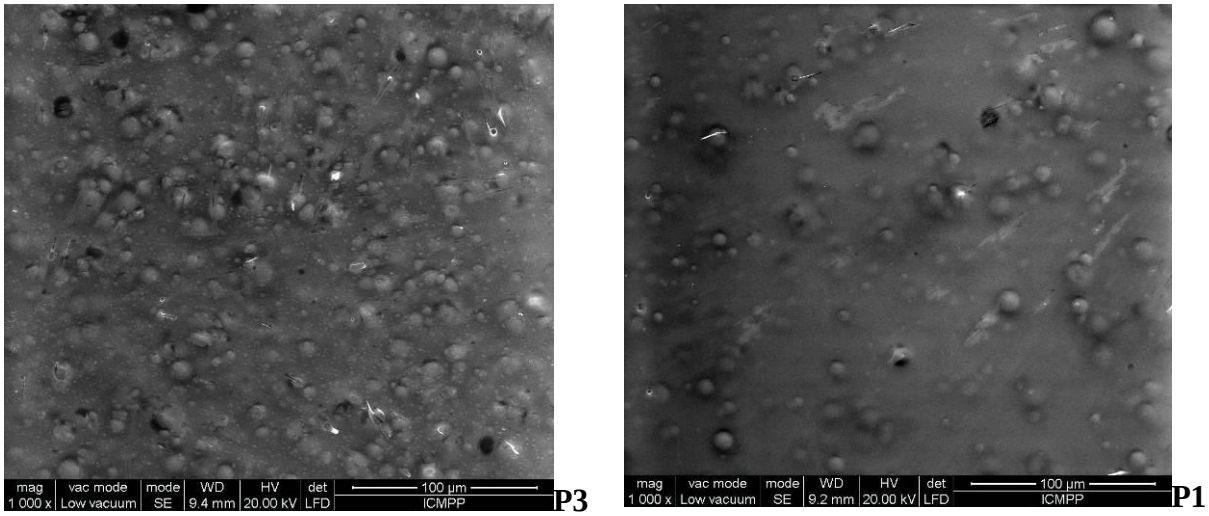

Figure 7. SEM microphotograph of PDLCs as obtained by casting

The film samples preheated at 80 ^{o}C, show round holes, which spatial distribution depends on the LC content: the holes are denser as the amount of LC increases (Figure 8a-d). Remarkable, the droplet diameter doesn't change significant as liquid crystalline percent increases, indicating no significant influence of the liquid crystal/polymer ratio upon the interphase forces which drive the droplet formation. As can be seen in figure 8a'-d', which represents the diameter size distribution and standard deviation value, the droplet diameter is comprised in the range 4 – 11 μm, with predominant droplet population around 7 μm. It could be observed that increasing of the liquid crystal amount into polymeric matrix is accompanied by the decreasing of the standard deviation indicating the narrower size polydispersity of the formed droplets.

Systematic studies of PDLC composites proved that devices with good electro-optic performance were obtained for micrometric droplets with diameter size less 10 μm, which assure a good balance between the transmittance and scattering of the incident light [35-37]. Moreover, it was demonstrated that PDLCs containing higher concentration of liquid crystal droplets enhance the device stability, while micrometric droplets which are able to preserve the intrinsic properties of the pure liquid crystal allow a good transmission of bistable states [13]. Taking into consideration all these, it can be observed that the understudy composites

meet the morphological features required by the high performance PDLC materials addressed to electro- optical devices, even of the bistable devices.

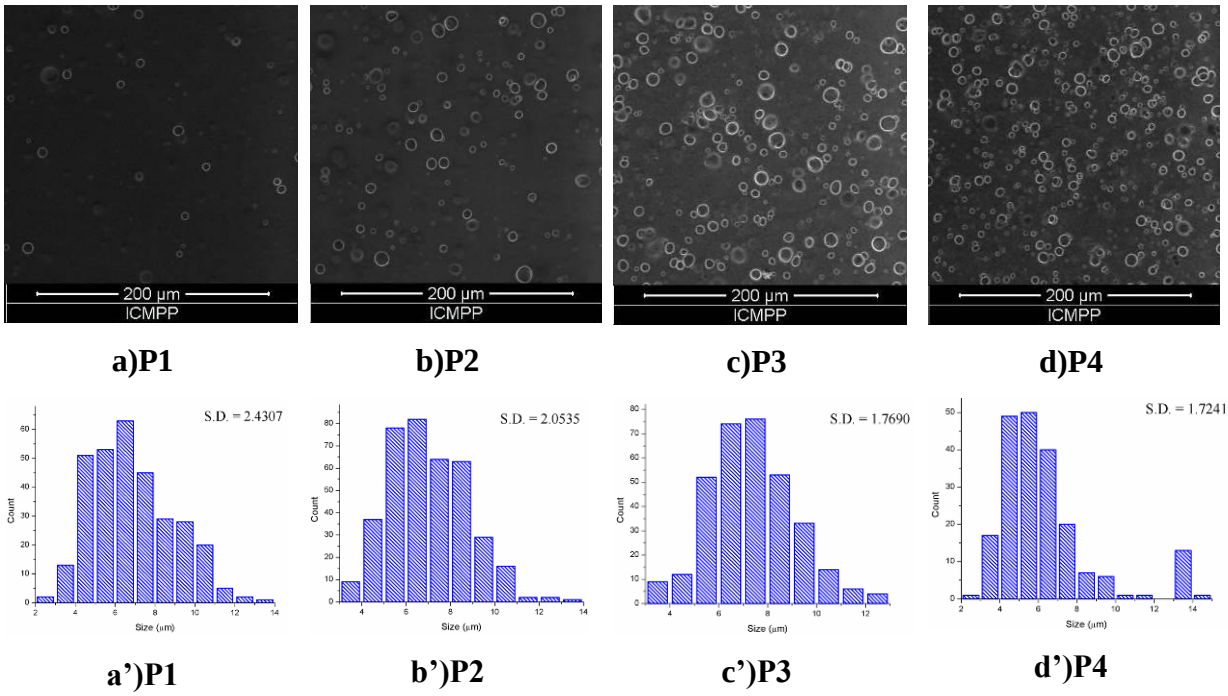

Figure 8. SEM microphotograpgh of **a**, **b**, **c**, **d**) preheated PDLCs and their **a'**, **b'**, **c'**, **d'**) corresponding particles mean size distribution and the values of the standard deviation (S.D.)

3.7.Hydrophilicity and surface free energy calculation

As a matter of fact, the surface properties of a biomaterial are essential characteristics which define its behaviour in a biological environment, and thus its potential for a good host-implanted integration. Important parameters which are usually considered when level of biocompatibility of a biomaterial is evaluated are the contact angle and the surface free energies. Exhaustive studies have demonstrated that biomaterials with moderate wettability / hydrophilicity - which correspond to a water contact angle value comprised in the range 60 - 90 degree, elicit the least foreign-body reactions for long term implantations [38]. On the other hand, in the case of ocular applications (lenses, artificial cornea) the biomaterial must have a water contact angle value close to that of natural cornea which is 50 degree [39]. Moreover, studies on PVA indicated that the contact angle value varies as a function of the crystallinity degree, offering the possibility to modulate the addressed application. This is an important feature, taking into consideration that POM and DSC measurements indicates the ability to tune the PVAB confinement matrix crystallinity.

In the light of these data, the water contact angle of the two pure components and their PDLC composites has been measured on the same films at different times after their preparation: 2 weeks and 4 months. As can be seen in figure 9, the contact angle of the pure **BBO** and **PVAB** film was not significantly affected by time, while that of the PDLC composites decreases as the liquid crystal content increases, reaching differences of 7 degrees in the case of **P4**. This behaviour is in agreement with the increasing of the crystallinity degree of the polymer matrix when the hydroxyl group density on its surface increases [39]. The crystallinity degree increases more for a higher BBO/PVAB weight ratio, due to the larger interphase surface which determines a more efficient coupling of the ordering at the interface between the two components.

The water contact angle value of the **BBO** and **PVAB** pure components indicate moderate hydrophilicity, both materials being potential biocompatible. By combining them into PDLC composites, the water contact angle value lays under moderate wettability for smaller amounts of **BBO** (**P1**, **P2**), but reach moderate hydrophilicity for higher **BBO** amount (**P3**, **P4**). Taking into consideration that higher droplet density is desirable for PDLC applications, these results suggest that **P3**, **P4** composite films are potential candidates for indwelling biomedical applications. On the other hand, the decreasing of the contact angle of the **P2** and **P3** films at values close to that of corneal surface indicate them as potential candidates for ocular biomedical applications. Consideration that the decreasing of the water contact angle is accompanied by the increasing of the crystallinity degree (as POM and DSC measurements proved) which means improved mechanical properties, their value for this kind of applications is realistic.

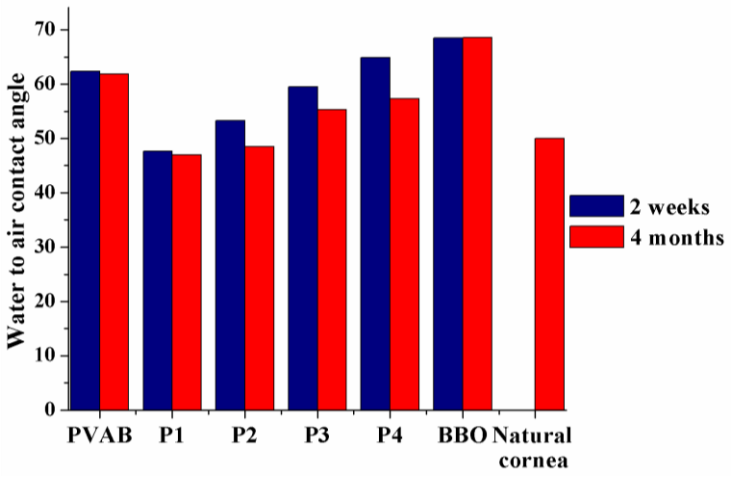

Figure 9. Mean static contact angles determined by sessile drop method

Surface free energy (SFE) is a surface property which reflects the chemical composition of the material and even molecule orientation, aspect especially important in the case of PDLC systems in which molecules inside the liquid crystal droplets are anchored within PDLC matrix by interphase forces. Total surface free energy (γ_s^{TOT}), dispersive (γ_s^{LW}), polar (γ_s^{AB}), acidic (γs^+) and basic (γs^-) components of the surface free energy were calculated based on the contact angle at equilibrium between PDLCs surface and three pure liquids: twice distilled water, formamide and diiodomethane [12, 25].

It is expected that the interphase interaction at the liquid crystal-polymer boundary to determine the **BBO** configuration into PDLC droplets and on the other hand to influence the surface free energy, which can be further electrically switched and thus used to design biosensors as blood sensors and sperm testers [40]. Moreover, it was demonstrated that biomaterials with surface free energy higher than 22 mN/m favour the cellular adhesion and maintains tissue multicellular structure [38, 41].

As can be seen in figure 10a, pure PVAB film has pretty high surface energy value of 47.46 mN/m, with an important contribution of dispersive Lisfshitz – van der Waals (γ_S^{LW} =37), and polar (γ^a = 10.46) forces given by the significant electron donating (γ_S^-=11.58) and less important electron accepting (γ_S^+=2.36) contributions. As expected, these results indicate much larger contribution of basic sites (attributed to the electron rich oxygen atoms) compared to acidic ones (attributed to electron deficient boron atoms), due to the higher number of rich electron oxygen atoms against electron deficient boron ones into the PVAB macromolecules.

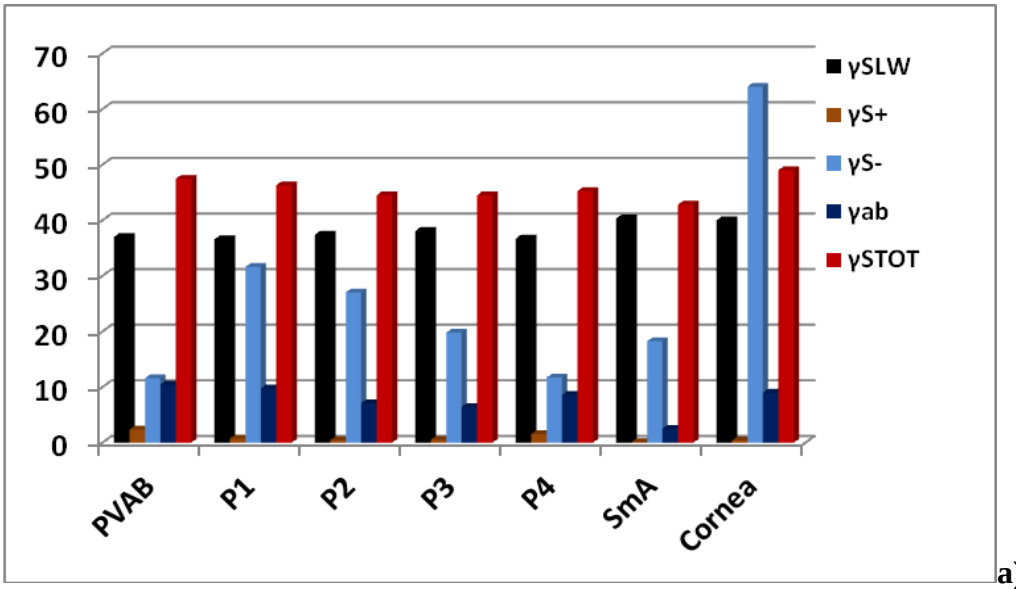

a)

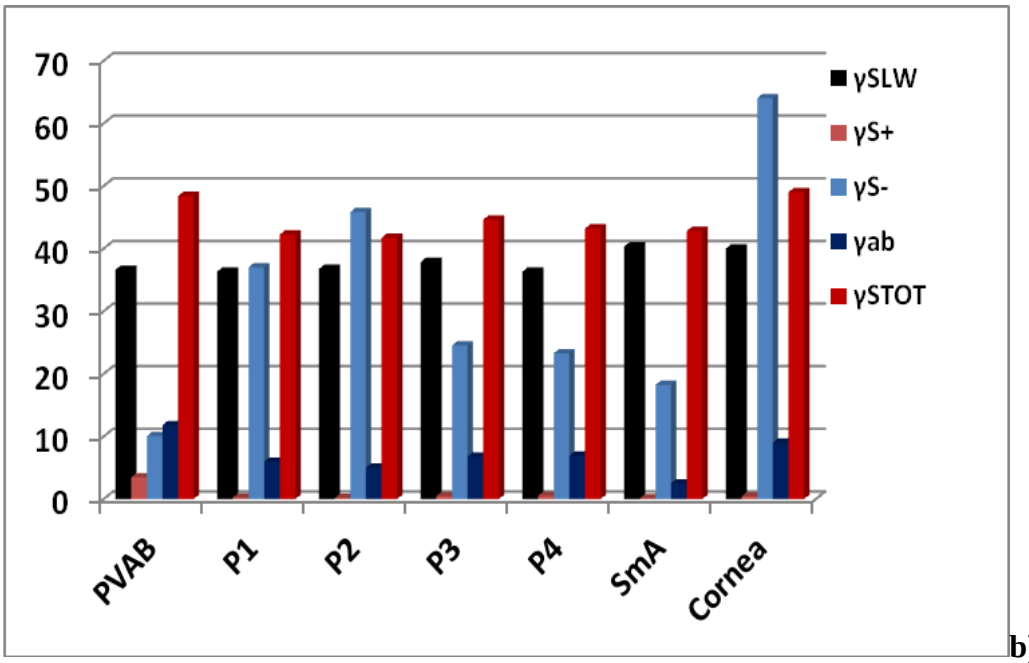

b)

Figure 10. The values of SFE and its components in mN/m of the films, a) 2 weeks and b) four months, after preparation

The **BBO** liquid crystal based on benzoate units has also high surface energy value of 42.8 mN/m, given by higher dispersive Lisfshitz – van der Waals contribution (γ_S^{LW} =40.32) and less important polar forces (γ^a =2.48) as result of almost missing electron accepting (γ_S^+=0.08) contributions despite of important electron donating (γ_S^-=18.22) contribution. This is in agreement with the liquid crystal structure consisting in rich electron donating ester groups and extremely weak electron donating nonpolar aliphatic units.

Compared to the PVAB matrix, the major surface free energy changes of PDLCs reside from the changes of the polar (γ^{ab}) contributions given by acidic (γs^+) and basic (γs^-) parts, the Lifshitz-Van der Walls component (γ_S^{LW}) being less affected by **BBO** liquid crystal addition into PVAB matrix, meaning that the BBO and the PVAB interacts mainly through hydrogen bonds and Lewis acid-base forces (Figure 10). Considering the acid-base theory, the boron from PAVB works as a Lewis acid (electron acceptor), whereas the hydroxyl group from PVAB and ester group from LC works as a Lewis base (electron donor).

The polar part γ^{ab} and Lewis acid γ^+ decrease while Lewis base γ^- component increases with increasing the **BBO** content in the **PDLC** composites, according with the interfacial interaction between **PVAB** and **BBO** which involves the predominant basic sites of **BBO** (COO) and acidic sites of **PVAB** (B) which renders more predominant OH basic sides of the PVAB to the interface.

Analysing the surface forces of the films kept four months (Figure 10b), it can be seen that acidic sites (boron atoms) contribution decreased even more almost disappearing, accompanied by the increasing of the basic sites contribution (OH). This fact confirms rearrangements of the PVAB macromolecules around the BBO droplets which affect the composite surface. Thus, during the time, more boron acidic sites orient to the BBO-PVAB interface, leading to the increasing of OH basic sites density accessible at the composite surface. The matrix and LC interacts through electron deficient boron and electron enriched ester group while hydroxyl groups from PVAB are being oriented towards the surface thus, the Lewis base component of SFE increases. No significant changes of the nonpolar sites can be seen, indicating insignificant Van der Waals interaction at the interface.

Comparing the surface energy values of the PDLC composites with those of natural cornea [39], close values of the total surface energy and its apolar and polar components can be seen, indicating once again the potential of the understudy materials for biological applications.

Conclusions

The obtaining of polymer dispersed liquid crystals based on a new smectogen and polyvinylalcohol-boric acid as polymer matrix revealed the ability of PVAB to constrain the growing of liquid crystal into smectic droplets. PVAB is a biocompatible polymer, soluble only in hot water, transparent, immiscible with liquid crystals, assuring good optical properties. The new smectic liquid crystal has a direct isotropic – smectic transition and forms a smectic A mesophase which is stable on a large temperature range (69 – 28 ^{o}C), superposed with that of the human body. The use of the PVAB as matrix succeeded in embedding of the smectic liquid crystal as planar anchored droplets due to the interfacial attractive forces between the electron deficient boron and electron rich ester units. The resulted PDLC films present a uniform distribution of the smectic droplets with narrow size polydispersity and diameter around 7 μm – ideal dimensional parameters for opto-electronic applications. The two components are completely immiscible fact which points for the advantage to keep their optical properties and precludes the lost of liquid crystal as plasticizer of the matrix. The value of surface free energy of the PDLC films is enough high to assure the electrically switching and cell adhesion. Moreover, the hydrophilicity of the PDLC films can be tuned by simple control of PVAB matrix morphology, to met requirements of different biological

applications. All these findings recommend the studied PDLC as materials for biomedical engineering.

Acknowledgements

The research leading to these results has received funding from the Romanian National Authority for Scientific Research, MEN – UEFISCDI grant, project number PN-II-PT-PCCA-2013-4-1861 (contract number 272/2014) and project number PN-II-ID-PCCE-2011-2-0028.

Supporting Information

The Raman spectra of pure **BBO** liquid crystal and **PVAB** matrix; Dependence of the intensity of the 1600 cm^{-1} Raman band on the rotation of the direction of the incident laser polarization; Raman images constructed from different spectral regions and their dependence on laser polarization, as indicated on the top and left of the figure; UV-vis and b) luminescence spectra of the pure LC and PDLC composites.

References

1. Drzaic P, Drzaic PS. Putting liquid crystal droplets to work: a short history of polymer dispersed liquid crystals. Liq. Cryst. 2006;33:1281–1296.

2. Bronnikov S, Kostromin S, Zuev V. Polymer - dispersed liquid crystals: progress in preparation, investigation, and application. J. Macromol. Sci. Phy. 2013;52:1718–1735.

3. Dierking I. Polymer Network–Stabilized Liquid Crystals. Adv. Mater. 2000;12:167–181.

4. Kitzerow HS. Polymer-dispersed liquid crystals from the nematic curvilinear aligned phase to ferroelectric films. Liq. Cryst. 1994;16:1–31.

5. Smith GW. Mixing and Phase Separation in Liquid Crystal Matrix System. Int. J. Mod Phys B. 1993;7:4187–4213.

6. Bouteiller L, Le Barny P. Polymer-dispersed liquid crystals: Preparation, operation and application. Liq. Cryst. 1996;21:157–174.

7. Sorrentino A, Gorrasi G, Vittoria V. Potential perspectives of bio-nanocomposites for food packaging applications. Trends Food Sci. Tech. 2007;18: 84–95.

8. Hsu TC, Lu CH, Huang YT, et al. Concentric polymer-dispersed liquid crystal rings for light intensity modulation. Sensor. Actuat. A-Phys. 2011;169:341–346.

9. Lapointe J, Durette JF, Harhira A, et al. 'Living' prosthetic iris. Eye. 2010;24:1716–1723.

10. Sidiq S, Das D, Pal SK. A new pathway for the formation of radial nematic droplets within a lipid-laden aqueous-liquid crystal interface. RSC Adv. 2014;4:18889–18893.
11. Woltman SJ, Jay GD, Crawford GP. Liquid-crystal materials find a new order in biomedical applications. Nat. Mater. 2007;6:929–938.
12. Marin L, Ailincai D, Paslaru E. Monodisperse PDLC composites generated by use of polyvinyl alcohol boric acid as matrix. RSC Adv. 2014;4:38397–38404.
13. Lu Y, Wei J, Shi Y, et al. Effects of fabrication condition on the network morphology and electro-optical characteristics of polymer-dispersed bistable smectic A liquid crystal device. Liq. Cryst. 2013;40:581–588.
14. Yonezawa J, Martin SM, Macosko CW, et al. Rheology and Morphology of Smectic Liquid Crystal/Polymer Blends. Macromolecules. 2004;37:6424–6432.
15. Date M, Takeuchi Y, Kato K. Droplet size effect on the memory-mode operating temperature of smectic-A holographic polymer dispersed liquid crystal. J. Phys. D: Appl. Phys. 1999; 32:3164–3168.
16. Soule ER, Abukhdeir NM, Rey AD. Thermodynamics, transition dynamics, and texturing in polymer-dispersed liquid crystals with mesogens exhibiting a direct isotropic/smectic-A transition. Macromolecules. 2009;42:9486–9497.
17. Kim J, Han JI. Effect of liquid crystal concentration on electro-optical properties of polymer dispersed liquid crystal lens for smart electronic glasses with auto-shading and auto-focusing function. Electron. Mater. Lett. 2014;10:607–610.
18. Lu Y, Wei J, Shi Y, et al. Effects of fabrication condition on the network morphology and electro-optical characteristics of polymer-dispersed bistable smectic A liquid crystal device. Liq. Cryst. 2013;40:581–588.
19. Jeon YJ, Lee GH, Jang JE, et al. Applications of multidirectional reflective light-control films on reflective polymer-dispersed liquid crystal displays for enhancement in image quality at lower viewing angles. Liq. Cryst. 2012;39:1314–1319.
20. Tu Y, Gu Y, Van Horn RM, et al. A synthetic approach towards micron-sized smectic liquid crystal capsules via the diffusion controlled swelling method. Polym. Chem. 2015; 6:2551–2559 and references herein.
21. Chen DY, Qiang YZ. Beyond displays: The recent progress of liquid crystals for bio/chemical detections. Chin. Sci. Bull. 2013;58:2557–2562.

22. Hwang JJ, Iyer SN, Li LS, et al. Self-assembling biomaterials: liquid crystal phases of cholesteryl oligo(L-lactic acid) and their interactions with cells. Proc. Natl. Acad. Sci. USA, 2002; 99:9662–9667.
23. Doshi AV, Joshi CG, Bhoya UC. Synthesis and study of Ester Mesogenic Homologous Series: Ethyl-o-[p'-n-alkoxy benzoyloxy]benzoates. Der Pharma Chemica. 2011;3:185–190.
24. Ailincai D, Marin L, Shova S, et al. Benzoate liquid crystal with direct isotropic-smectic transition and antipathogenic activity. CR Chim. 2016 accepted
25. Van Oss CJ, Good RJ, Chaudhury MK. Additive and nonadditive surface tension components and the interpretation of contact angles. Langmuir. 1988;4:884–891.
26. Marin L, van der Lee A, Shova S, et al. Molecular amorphous glasses toward large azomethine crystals with aggregation-induced emission. New J. Chem. 2015;39:6404–6420.
27. Demus D, Richter L. Textures of Liquid Crystals. VEB Deutscher Verlag fur Grundstoffindustrie: Leipzig; 1980.
28. Liq Cryst – textura fan shaped pentru smectic A
29. Nicholas L, Abbott N, Christopher JM, et al. Engineering interfaces to cells using synthetic liquid crystals. Eur. Cells Mater. 2005; 10, CS1.
30. Luk Y, Yang KL, Cadwell K, et al. Deciphering the interactions between liquid crystals and chemically functionalized surfaces: Role of hydrogen bonding on orientations of liquid crystals. Surf. Sci. 2004;570:43–56.
31. Lovinger AJ, Amundson KR, Davis DD. Morphological investigation of UV-curable polymer-dispersed liquid-crystal (PDLC) materials. Chem. Mater. 1994;6:1726–1736.
32. Marin L, Popescu MC, Zabulica A, et al. Chitosan as a matrix for biopolymer dispersed liquid crystal systems. Carbohyd. Polym. 2013;95:16–24.
33. Hayashi N, Kato T, Aoki T, et al. Orientational distributions in smectic liquid crystals showing V-shaped switching investigated by polarized Raman scattering. Phys. Rev. E. 2002; 65:041714.
34. Lopez-Leon T, Fernandez-Nieves A. Drops and shells of liquid crystal. Colloid Polym Sci. 2011;289:345–359.
35. Li W, Cao Y, Cao H, et al. Control of the microstructure of polymer network and effects of the structures of polymerizable monomers on the electro-optical properties of uv- cured polymer dispersed liquid crystal films. J. Polym. Sci. B. 2008;46:1369–1375.
36. Drzaic PS. Liquid Crystal Dispersion. World Scientific: Singapore; 1995.

37.Ding X, Cao M, Liu H, et al. A study of electro-optical properties of PDLC films prepared by dual UV and heat curing, Liq Cryst. 2008; 35:587-595.
38. Ikada Y. Surface modification of polymers for medical applications. Biomaterials. 1994;15:726–736.
39. Jiang H, Zuo Y, Zhang L, et al. Property-based design: optimization and characterization of polyvinyl alcohol (PVA) hydrogel and PVA-matrix composite for artificial cornea. J. Mater. Sci. Mater. Med. 2014; 25:941–952.
40. Lin YH, Chu TY, Tsou YS, et al. An electrically switchable surface free energy on a liquid crystal and polymer composite film. Appl. Phys. Lett., 2012;101:233502.
41. Hallab N, Bundy K, O'Connor K, et al. Evaluation of metallic and polymeric biomaterial surface energy and surface roughness characteristics for directed cell adhesion. Tissue. Eng. 2001;7:55–71.